# Renormalized interactions with a realistic single-particle basis

Angelo Signoracci,[1] B. Alex Brown,[1] and Morten Hjorth-Jensen[2]
[1]*Department of Physics and Astronomy and National Superconducting Cyclotron Laboratory, Michigan State University, East Lansing, Michigan 48824-1321, USA*
[2]*Department of Physics and Center of Mathematics for Applications, University of Oslo, N-0316 Oslo, Norway*
(Received 27 September 2010; revised manuscript received 25 January 2011; published 28 February 2011)

Neutron-rich isotopes in the $sdpf$ space with $Z \leqslant 14$ require modifications to derived effective interactions to agree with experimental data away from stability. A quantitative justification is given for these modifications because of the weakly bound nature of model space orbits via a procedure using realistic radial wave functions and realistic $NN$ interactions. The long tail of the radial wave function for loosely bound single-particle orbits causes a reduction in the size of matrix elements involving those orbits, most notably for pairing matrix elements, resulting in a more condensed level spacing in shell-model calculations. Example calculations are shown for $^{36}$Si and $^{38}$Si.

DOI: 10.1103/PhysRevC.83.024315 PACS number(s): 21.60.Jz, 21.60.Cs

## I. INTRODUCTION

New facilities for rare isotope beams will push the experimental capabilities of nuclear physics with radioactive beams to more unstable, shorter-lived nuclei. Properties of these nuclei exhibiting different behavior than stable nuclei, like the evolution of shell structure, are of significant interest for the next decades of research. A new theoretical technique and its behavior for stable and exotic nuclei was studied to examine the importance of refining theoretical approaches for the production of model space interactions for unstable nuclei.

Much research was done using renormalization methods to convert a realistic interaction fit to nucleon-nucleon ($NN$) scattering data into an interaction in the nuclear medium. The goal was to renormalize the interaction to valence orbits outside of a stable, semimagic or doubly magic nucleus treated as a vacuum in further calculations. A typical example would use $^{16}$O as the core and renormalize the $NN$ interaction into the $sd$ model space. For such an application, the harmonic oscillator basis of the form $\Psi_{nlm_l}(\vec{r}) = R^{\mathrm{HO}}_{nl}(\mathrm{r})\ Y_{lm_l}(\theta,\phi)$ is generally used, where all the valence orbits are bound. For more exotic closed-subshell nuclei, loosely bound orbits often play a role. Loosely bound orbits particularly deviate from the oscillator basis, as they exhibit a "long-tail" behavior with a larger spread in the radial wave functions. The harmonic oscillator basis is therefore less applicable further from stability. However, few calculations have been done with a realistic radial basis for unstable nuclei with renormalized $NN$ interactions.

Experimental interest in neutron-rich silicon isotopes and the failure of some shell-model Hamiltonians to reproduce data in the region have led to modifications in the SDPF-NR interaction [1], which had been the standard for shell-model calculations in the $sdpf$ model space. The new SDPF-U interaction has different neutron-neutron pairing matrix elements for $Z \geqslant 15$ and $Z \leqslant 14$ to account for the behavior of $pf$ neutron orbits relative to the number of valence protons. The $Z \leqslant 14$ version of the interaction treats neutron-rich unstable nuclei that exhibit different shell behavior than the less exotic nuclei in the $Z \geqslant 15$ nuclei. The interest in silicon isotopes and the nature of the SDPF-U interaction make $^{34}$Si a suitable choice for the renormalization procedure with a realistic basis. A similar effect occurs for the neutron-rich carbon isotopes around the $N = 14$ closed subshell, requiring a 25% reduction in the neutron-neutron two-body matrix elements from the effective interactions derived for the oxygen isotopes [2].

## II. RENORMALIZATION PROCEDURE

We begin with the realistic charge-dependent $NN$ interaction N$^3$LO derived at fourth order of chiral perturbation theory with a 500-MeV cutoff and fit to experimental $NN$ scattering data [3]. The N$^3$LO interaction is renormalized using a similarity transformation in momentum space with a sharp cutoff of $\Lambda = 2.2\ \mathrm{fm}^{-1}$ to obtain the relevant low momentum interaction [4]. We will refer to this technique as a $v_{\mathrm{lowk}}$ renormalization. Skyrme Hartree-Fock calculations are performed with the Skxtb interaction [5] for a chosen closed subshell target nucleus to determine the binding energy, single-particle radial wave functions, and single-particle energy spectra for neutrons and protons of the target nucleus. Although the low momentum interaction could be used in a Hartree Fock calculation, it would not include the essential effective one-body component of the three-body (and higher) terms of the interaction. The low momentum interaction is then renormalized into a model space of interest using Rayleigh-Schrödinger perturbation theory [6] to second order including excitations up to $6\hbar\omega$, summing over folded diagrams to infinite order. We will compare three options for the renormalization to produce an effective interaction: harmonic oscillator single-particle energies and wave functions (HO), Skyrme Hartree-Fock single-particle energies and wave functions (SHF), and Skyrme Hartree-Fock single-particle energies and harmonic oscillator single-particle wave functions (CP).

The CP basis and HO basis give identical results to first order in perturbation theory because they use identical wave functions. The energies, which are different in the two procedures, come into higher order diagrams via energy denominators, as discussed in [6]. Therefore, the last option is a core-polarization basis (CP basis) because the

 

core-polarization diagrams are affected to leading order even though the result at first order is unchanged.

Skyrme Hartree-Fock radial wave functions, once solved, are implemented in the renormalization by using an expansion in terms of the harmonic oscillator basis via

$$\psi^{\rm SHF}_{nlj}(\vec{r}) = \sum_n a_n R^{\rm HO}_{nl}(r)[Y_l(\theta,\phi)\otimes\chi_s]_j, \qquad (1)$$

where $a_n^2$ gives the percentage of a specific harmonic oscillator wave-function component in the Skyrme Hartree-Fock wave function. The Skyrme Hartree-Fock wave functions and single-particle energies can only be determined for bound states. For unbound orbits, the harmonic oscillator basis remains in use, but the Gram-Schmidt process is used to ensure orthonormality of the single-particle wave functions. The effective interaction, consisting of the derived two-body matrix elements and the Skyrme Hartree-Fock single-particle energies, can then be used in a shell-model program directly.

## III. APPLICATION TO SDPF MODEL SPACE

Neutron-rich silicon isotopes present an interesting application of the procedure outlined in the last section. A deeper understanding of the need for multiple interactions in the $sdpf$ model space, as seen by the form of SDPF-U, can be gained by performing the renormalization for the same model space in multiple ways. The model space chosen is the $sd$ proton orbits and $pf$ neutron orbits. The renormalization procedure is done using all three options for two different target nuclei, producing a total of six interactions. The two target nuclei chosen are the stable $^{40}$Ca doubly magic nucleus, and the neutron-rich $^{34}$Si semimagic nucleus. Single-particle energies of the SHF basis, using the Skxtb interaction, are presented in Table I for both target nuclei. For an SHF state that is unbound, the radial wave function is approximated by a state bound by 200 keV that is obtained by multiplying the SHF central potential by a factor larger than unity. The energy of the unbound state is estimated by taking the expectation value of this bound-state wave function in the original SHF potential.

TABLE I. Single-particle energies for $^{34}$Si and $^{40}$Ca using the Skxtb interaction. Values in bold are in the model space.

| $nl_j$ | $^{34}$Si Proton | $^{34}$Si Neutron | $^{40}$Ca Proton | $^{40}$Ca Neutron |
|---|---|---|---|---|
| $0s_{1/2}$ | −37.73 | −32.79 | −30.49 | −38.18 |
| $0p_{3/2}$ | −27.60 | −23.10 | −22.14 | −29.70 |
| $0p_{1/2}$ | −22.39 | −21.74 | −19.03 | −26.67 |
| $0d_{5/2}$ | **−17.29** | −13.07 | **−12.79** | −20.20 |
| $0d_{3/2}$ | **−9.08** | −9.03 | **−7.23** | −14.65 |
| $1s_{1/2}$ | **−13.49** | −10.04 | **−8.31** | −15.75 |
| $0f_{7/2}$ | −5.97 | **−2.62** | −2.68 | **−9.89** |
| $0f_{5/2}$ | 3.70 | **3.33** | 4.81 | **−2.43** |
| $1p_{3/2}$ | −1.06 | **−0.40** | 1.44 | **−5.48** |
| $1p_{1/2}$ | 1.49 | **−0.27** | 3.27 | **−3.66** |
| $0g_{9/2}$ | 6.39 | 9.22 | 8.63 | 1.15 |
| $0g_{7/2}$ | 18.26 | 18.23 | 18.76 | 10.28 |

TABLE II. Single-particle energies for $^{34}$Si and $^{40}$Ca in the harmonic oscillator basis. The energy shift is chosen so that the valence energy is identical in both bases. Values in bold are in the model space.

| $nl_j$ | $^{34}$Si Proton | $^{34}$Si Neutron | $^{40}$Ca Proton | $^{40}$Ca Neutron |
|---|---|---|---|---|
| $0s_{1/2}$ | −36.93 | −34.59 | −32.22 | −39.21 |
| $0p_{3/2}$ | −25.42 | −23.09 | −21.20 | −28.19 |
| $0p_{1/2}$ | −25.42 | −23.09 | −21.20 | −28.19 |
| $0d_{5/2}$ | **−13.91** | −11.58 | **−10.18** | −17.17 |
| $0d_{3/2}$ | **−13.91** | −11.58 | **−10.18** | −17.17 |
| $1s_{1/2}$ | **−13.91** | −11.58 | **−10.18** | −17.17 |
| $0f_{7/2}$ | −2.40 | **−0.07** | 0.84 | **−6.15** |
| $0f_{5/2}$ | −2.40 | **−0.07** | 0.84 | **−6.15** |
| $1p_{3/2}$ | −2.40 | **−0.07** | 0.84 | **−6.15** |
| $1p_{1/2}$ | −2.40 | **−0.07** | 0.84 | **−6.15** |
| $0g_{9/2}$ | 9.11 | 11.44 | 11.86 | 4.87 |
| $0g_{7/2}$ | 9.11 | 11.44 | 11.86 | 4.87 |

In the SHF basis, the calculation of single particle energies shows that the proton orbits are shifted down in energy for $^{34}$Si relative to $^{40}$Ca, whereas the neutron orbits are shifted up. For the valence neutrons, this shift results in a switch from four orbits for $^{40}$Ca bound by 5.4 Mev on average to four orbits for $^{34}$Si centered at 0.0 MeV. This change, specifically the loosely bound energies of the $p_{3/2}$ and $p_{1/2}$, has a significant effect on the wave functions, which will be discussed in more detail later. For comparison, the single-particle energies used in the HO basis are given in Table II. The Blomqvist-Molinari formula [7] $\hbar\omega = (45A^{-1/3} - 25A^{-2/3})$ MeV gives 11.508 MeV for $A = 34$ and 11.021 MeV for $A = 40$. The absolute value of the harmonic oscillator basis is irrelevant, as only energy differences come into the diagrams in Rayleigh-Schrödinger perturbation theory. For a better comparison to the SHF basis, the absolute value is chosen separately for protons and neutrons such that $\sum_1^{n_{\rm val}}(2J+1)\epsilon_\alpha$ is identical in the HO and SHF bases, where $n_{\rm val}$, the number of valence orbits, is three for protons and four for neutrons and $\epsilon_\alpha$ is the energy of the single-particle orbit given by the $\alpha = n, l, j$ quantum numbers. To avoid divergences from the calculation of energy denominators, all model space orbits are set to the same valence energy such that the starting energy [6] of each diagram is constant.

Figure 1 shows a comparison of the $pf$ matrix elements in MeV for both target nuclei with the HO basis used in the renormalization procedure. The values deviate slightly from the line of equality but agree well with each other. Therefore, the choice of target nucleus, whether $^{34}$Si or $^{40}$Ca, has little effect on the matrix elements in the HO basis. However, in Fig. 2, where the comparison is for both target nuclei in the SHF basis, a reduction in the strength of the interaction for $^{34}$Si is observed. This reduction with $^{34}$Si as the target nucleus is because of the weakly bound nature of the $pf$ neutron orbits.

In the SHF basis, the $f_{7/2}$ orbit is bound by 2.6 MeV, and its radial wave function agrees reasonably well with the harmonic oscillator wave function as seen in Fig. 3. The Skyrme wave function is expanded in the harmonic oscillator basis up to $n = n_{\rm max}$ and the $a_n$ coefficients are renormalized to ensure

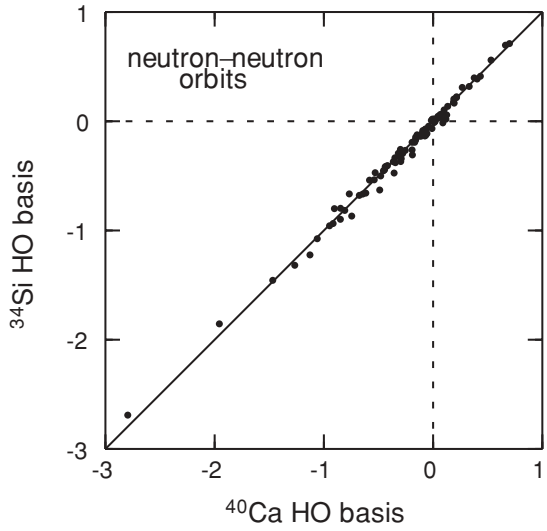


FIG. 1. Comparison of $pf$ neutron-neutron matrix elements (in MeV) for the renormalization procedure in the HO basis for the two target nuclei. The solid line $y = x$ denotes where the matrix elements would be identical.

that $\sum_{n=0}^{n_{\max}} a_n^2 = 1$. For our renormalization procedure, orbits up to $(2n + l) = 9$ are included, which gives $n_{\max} = 3$ for the $f_{7/2}$ and $f_{5/2}$ orbits and $n_{\max} = 4$ for the $p_{3/2}$ and $p_{1/2}$ orbits. This includes over 99% of the strength for the $f$ orbits, but only 93% and 92% for the $p_{3/2}$ and $p_{1/2}$ orbits, respectively. A first-order calculation can be done to $n_{\max} = 6$ for all orbits, which gives 100%, 98%, and 97% for the $f$, $p_{3/2}$, and $p_{1/2}$ expansions, respectively.

With this procedure, 99% of the $f_{7/2}$ orbit is represented by the $R_{03}^{\mathrm{HO}}$ wave function, but the 1% represented by $R_{23}^{\mathrm{HO}}$ and

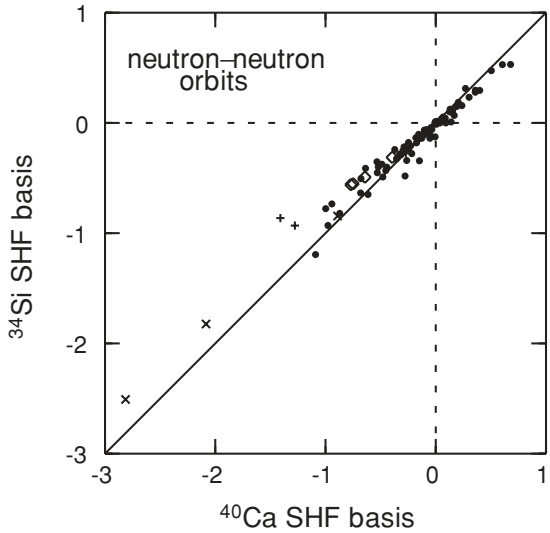


FIG. 2. Comparison of $pf$ neutron-neutron matrix elements (in MeV) for the renormalization procedure in the SHF basis for the two target nuclei. The solid line $y = x$ denotes where the matrix elements would be identical. Black dots correspond to matrix elements with $J > 0$, whereas the $J = 0$ matrix elements are split into three groups: $ff$-$ff$ (crosses), $ff$-$pp$ (diamonds), and $pp$-$pp$ (plus signs).

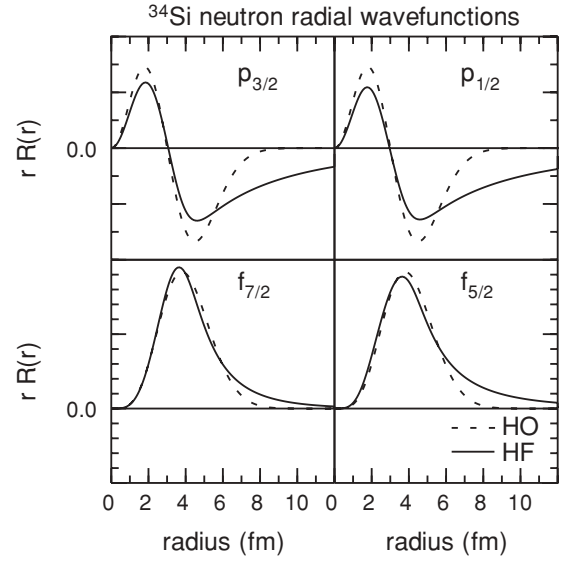


FIG. 3. Comparison of the single-particle radial wave functions for $^{34}$Si in the HO and SHF bases.

$R_{33}^{\mathrm{HO}}$ has a significant effect at large radii. The $p_{3/2}$ and $p_{1/2}$ orbits are only bound by 400 and 269 keV, respectively. The expected harmonic oscillator component $R_{11}^{\mathrm{HO}}$ only makes up 80% and 78% of the respective radial wave functions. Higher $n$ orbits that extend farther away from the center of the nucleus contribute the remaining strength. The $f_{5/2}$ orbit is unbound by 3 MeV, but the solution for the Skyrme radial wave function is determined by assuming that the orbit is bound by 200 keV. With this method, 97% of the realistic radial wave function is given by the $R_{03}^{\mathrm{HO}}$ wave function. Single-particle radial wave functions of valence space neutron orbits are shown in Fig. 3 in both the HO and SHF bases. The long tail behavior of the realistic basis is evident, as the wave functions have significant strength beyond 8 fm unlike the oscillator wave functions, especially for the loosely bound $p$ orbits.

The $J = 0$ matrix elements in Fig. 2 deviate more from the line of equality (i.e., the pairing matrix elements are reduced for $^{34}$Si when the N$^3$LO interaction is renormalized in the SHF basis). The SDPF-U interaction has different neutron-neutron pairing matrix elements for $Z \geqslant 15$ and for $Z \leqslant 14$ to account for $2p$-$2h$ excitations of the core correctly, depending on whether $^{34}$Si or $^{40}$Ca should be considered the core [1]. The SDPF-U neutron-neutron pairing matrix elements are reduced by 300 keV for $Z \leqslant 14$ to produce results in better agreement with experimental data. The pairing matrix elements in Fig. 2 are reduced for the $^{34}$Si target by 214 keV on average, relative to the case with $^{40}$Ca as the target. Although the connection here to the $Z$ dependence in SDPF-U is only suggestive, the change in target mimics the change in core for calculations in the $sdpf$ region, cited by Nowacki and Poves as the cause of their 300-keV reduction [1]. The reduction of 214 keV is solely because of the change in occupation of the $d_{5/2}$ proton orbit, which can affect the single-particle energies and radial wave functions, as well as the available orbits in second-order diagrams. We find that the change in single-particle radial wave functions plays the most significant role, but we are also able to analyze the other effects.

TABLE III. First-order, particle-particle ladder, core-polarization, four-particle two-hole, and total matrix elements in MeV of the form $\langle aa|V|bb\rangle_{J=0}$ for different renormalization procedures.

| $a$ | $b$ | | $^{34}$Si | | | $^{40}$Ca | | |
|---|---|---|---|---|---|---|---|---|
| | | | HO | CP | SHF | HO | CP | SHF |
| $f_{7/2}$ | $f_{7/2}$ | First | −0.906 | −0.906 | −0.807 | −0.938 | −0.938 | −0.870 |
| | | 2$p$-ladder | −0.409 | −0.414 | −0.422 | −0.409 | −0.418 | −0.450 |
| | | Core polarization | −0.449 | −0.377 | −0.417 | −0.637 | −0.649 | −0.768 |
| | | 4$p$2$h$ | −0.376 | −0.442 | −0.435 | −0.374 | −0.434 | −0.499 |
| | | Total | −1.855 | −1.869 | −1.824 | −1.957 | −1.982 | −2.084 |
| $f_{7/2}$ | $p_{3/2}$ | First | −0.518 | −0.518 | −0.322 | −0.518 | −0.518 | −0.368 |
| | | 2$p$-ladder | −0.148 | −0.157 | −0.119 | −0.152 | −0.164 | −0.138 |
| | | Core polarization | −0.121 | −0.118 | −0.074 | −0.282 | −0.309 | −0.283 |
| | | 4$p$2$h$ | −0.123 | −0.141 | −0.104 | −0.126 | −0.142 | −0.143 |
| | | Total | −0.800 | −0.822 | −0.552 | −0.903 | −0.926 | −0.749 |
| $f_{7/2}$ | $p_{1/2}$ | First | −0.585 | −0.585 | −0.421 | −0.572 | −0.572 | −0.452 |
| | | 2$p$-ladder | −0.042 | −0.050 | −0.039 | −0.049 | −0.062 | −0.038 |
| | | Core polarization | −0.055 | −0.041 | −0.043 | −0.212 | −0.236 | −0.231 |
| | | 4$p$2$h$ | −0.057 | −0.058 | −0.037 | −0.062 | −0.060 | −0.052 |
| | | Total | −0.665 | −0.663 | −0.492 | −0.767 | −0.779 | −0.642 |
| $p_{3/2}$ | $p_{3/2}$ | First | −1.109 | −1.109 | −0.776 | −1.096 | −1.096 | −1.082 |
| | | 2$p$-ladder | −0.233 | −0.242 | −0.165 | −0.233 | −0.237 | −0.242 |
| | | Core polarization | −0.037 | 0.001 | 0.000 | −0.021 | −0.005 | −0.037 |
| | | 4$p$2$h$ | −0.085 | −0.093 | −0.057 | −0.090 | −0.098 | −0.109 |
| | | Total | −1.319 | −1.313 | −0.931 | −1.267 | −1.252 | −1.278 |
| $p_{3/2}$ | $p_{1/2}$ | First | −1.540 | −1.540 | −0.857 | −1.478 | −1.478 | −1.382 |
| | | 2$p$-ladder | −0.060 | −0.069 | −0.078 | −0.068 | −0.081 | −0.077 |
| | | Core polarization | 0.068 | 0.082 | 0.045 | −0.038 | −0.069 | −0.080 |
| | | 4$p$2$h$ | −0.048 | −0.051 | −0.026 | −0.053 | −0.054 | −0.056 |
| | | Total | −1.456 | −1.462 | −0.863 | −1.469 | −1.488 | −1.409 |

Table III isolates a few matrix elements and compares the total matrix elements and their various components for both target nuclei in all three bases. Three diagrams contribute at second order, denoted as core polarization, particle-particle ladder, and four-particle two hole [6]. The total matrix element is not a simple summation of the first- and second-order diagrams, as we include the folded diagram procedure [6]. The reduction for total matrix elements involving $p$ orbits in the SHF basis with $^{34}$Si as the core is dramatic (≈30%) and is primarily from the extension of wave-function strength to large distances. Kuo *et al.* [8] noted a reduction of core polarization in the harmonic oscillator basis and used different oscillator parameters to account for the core nucleons and valence nucleons separately in halo nuclei. Although $^{34}$Si is not a halo nucleus, the loosely bound $p$ orbits behave in much the same way as the valence nucleons in a halo nucleus. The reduction in core polarization is seen going from the $^{40}$Ca target to the $^{34}$Si target in any basis in Table III, although the size of the polarization is reduced for nucleons far from the core. As noted in Ref. [8], the core interacts less with nucleons far away, so the excitations of the core are reduced. The core polarization for matrix elements solely involving $p$ orbits is under 100 keV. Nowacki and Poves [1] attributed the reduction in neutron-neutron pairing matrix elements for the empirical SDPF-U interaction to a decrease in core polarization for the $^{34}$Si target. We observe that the core polarization can be reduced significantly without the total matrix element changing in the same proportion. For instance, the $\langle f_{7/2}f_{7/2}|V|f_{7/2}f_{7/2}\rangle$ matrix element is only reduced by 5% from $^{40}$Ca to $^{34}$Si in the HO basis even though the core polarization is reduced by 30%. In the SHF basis, which takes into account the realistic wave function, the total matrix element is reduced by 13% whereas the core polarization is reduced by 46%. We would prefer to compare matrix elements involving the $p_{3/2}$ or $p_{1/2}$ orbits, but the core polarization becomes very small for loosely bound orbits, skewing percentage comparisons. Ogawa *et al.* [9] produce results that seem to be consistent with ours, identifying a 10%–30% reduction in nuclear interaction matrix elements involving loosely bound orbits using a realistic Woods-Saxon basis. However, they were limited to comparisons of ratios of matrix elements and did not include core polarization. We show that core-polarization suppression and reduction from spread of the wave functions are both important effects that should be included, as well as the other diagrams that contribute at second order. The full treatment of the renormalization in a

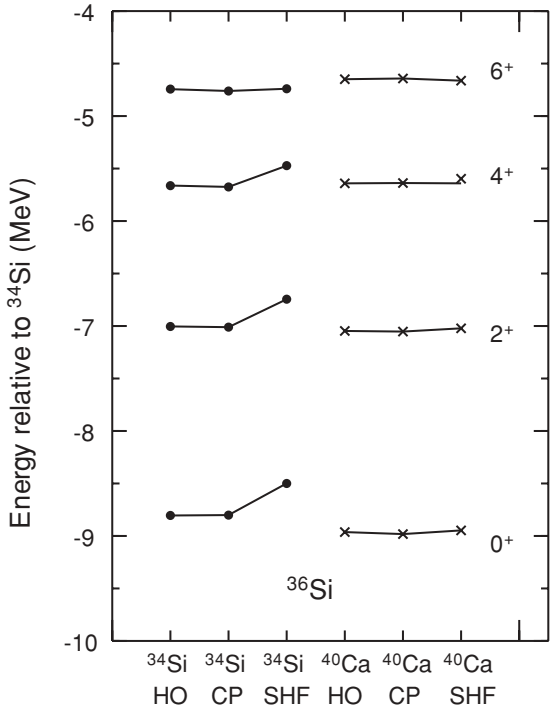


FIG. 4. Calculations of the lowest energy states for $J = 0, 2, 4, 6$ in $^{36}$Si relative to $^{34}$Si from the renormalization procedure for $^{34}$Si and $^{40}$Ca, in the HO, CP, and SHF bases for both target nuclei. Crosses are used for calculations with $^{40}$Ca as the target nucleus.

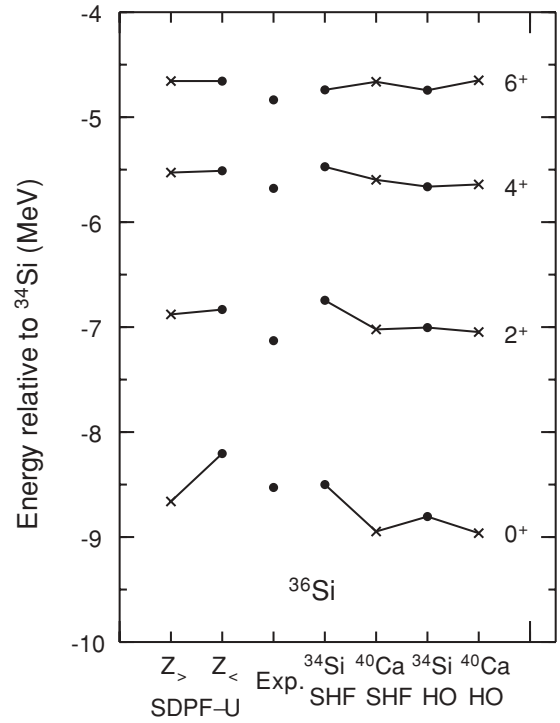


FIG. 5. Calculations of the lowest energy states for $J = 0, 2, 4, 6$ in $^{36}$Si relative to $^{34}$Si using the empirical SDPF-U interaction and the renormalization procedure for both $^{34}$Si and $^{40}$Ca as target nuclei, using the SHF and HO bases. Experimental data are shown for comparison, with a new mass from [11]. Crosses are used for calculations with $^{40}$Ca as the target nucleus.

realistic basis, as developed here, is necessary for accurate results. Our improvements enable us to perform calculations for neutron-rich silicon isotopes directly.

## IV. CALCULATIONS FOR $^{36}$SI AND $^{38}$SI

The effect of the different interactions on nuclear structure calculations was studied as neutrons are added to $^{34}$Si. To obtain a consistent starting point, the proton-proton and proton-neutron matrix elements of SDPF-U have been used, with proton single-particle energies (SPEs) chosen to reproduce those obtained by SDPF-U. Because SDPF-U does not reproduce the binding energy of $^{35}$Si, the SDPF-U neutron SPEs have been increased by 660 keV. The six interactions use neutron SPEs that reproduce the values of this modified SDPF-U interaction.

The only difference in the six interactions used in the calculations are the neutron-neutron matrix elements. Calculations have been done in the model space discussed in the last section with the shell-model code NUSHELLX [10]. Figure 4 shows the lowest $J = 0, 2, 4, 6$ states in $^{36}$Si, relative to $^{34}$Si. The HO basis and the CP basis for the same target nucleus deviate by no more than 20 keV. However, the SHF basis noticeably shifts the states, with the largest effect being 300 keV less binding in the ground state with $^{34}$Si as the target nucleus. The binding energy of $^{36}$Si changes by nearly 500 keV depending on which renormalization procedure is used. Furthermore, the level schemes for $^{36}$Si are more spread out for the crosses where $^{40}$Ca is chosen as the target nucleus.

Figure 5 shows the same states in $^{36}$Si relative to $^{34}$Si, but now the comparison includes the SDPF-U calculations and experimental data. The CP basis results are not included because they are so similar to the HO basis calculations. We see that the level scheme for $^{36}$Si is more spread out for the $Z \geqslant 15$ SDPF-U calculation than for the $Z \leqslant 14$ calculation, in agreement with our results discussed previously. Our calculations for each method are in reasonable agreement with the comparable SDPF-U calculation; the $0^+$ state differs most with about 300 keV more binding compared to the respective empirical interaction for each core. The experimental binding energy relative to $^{34}$Si is taken from a new mass measurement of $^{36}$Si, which is 140 keV higher in energy than previously measured [11]. The excitation energies of the $Z \leqslant 14$ SDPF-U calculation are comparable to experiment, as expected from an interaction fit specifically to neutron-rich silicon isotopes. Although no interaction reproduces the experimental data very well, general trends can be seen. The calculations with $^{40}$Ca as the target nucleus depicted by crosses result in level schemes that are too spread out in comparison to the experimental data. The reduction in the strength of the interaction for $^{34}$Si using the SHF basis results in a reduction of the energy of the states in $^{36}$Si, especially for the ground state (the pairing matrix elements were most reduced). The root mean square (rms) deviation between experiment and theory with $^{34}$Si as the target nucleus in the SHF basis is 223 keV for the four states shown. One reason for this deviation is the lack

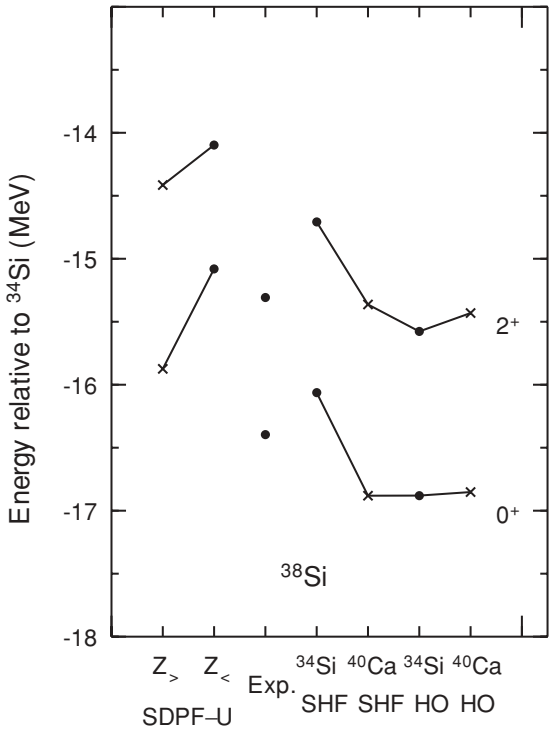


FIG. 6. Calculations for the lowest energy states for $J = 0$ and $J = 2$ in $^{38}$Si relative to $^{34}$Si using neutron-neutron matrix elements from SDPF-U and the renormalization procedure for both $^{34}$Si and $^{40}$Ca as target nuclei, using the SHF and HO bases. Crosses are used for calculations with $^{40}$Ca as the target nucleus.

of three-body forces in the procedure. The inclusion of the $NNN$ interaction, at least via the effective two-body part, is important for a higher level of accuracy. Additionally, the chosen SPEs may contribute to the deviation, which would be better constrained if all the single-particle states in $^{35}$Si were known experimentally. For exotic nuclei, the calculated single-particle state is often above the neutron separation energy and determination of the experimental single-particle states may not be possible with current facilities. Thus it is essential to improve energy density functionals such that they provide reliable single-particle energies.

As more nucleons are added, the disagreement between the various models increases as seen in Fig. 6, which plots the level scheme of $^{38}$Si relative to $^{34}$Si. Only the $0^+$ and $2^+$ states are shown because the $4^+$ and $6^+$ states are not known experimentally, but the binding energy is best reproduced by the calculations with $^{34}$Si in the SHF basis. As noted in the $^{36}$Si case, the excitation energy of the $2^+$ state is too high in the SHF basis but is reproduced well by the $Z \leqslant 14$ SDPF-U calculation for $^{38}$Si. Although the theoretical calculations of the binding energy vary by more than 750 keV for $^{36}$Si, the effect gets magnified as more particles are added. The binding energy of $^{38}$Si varies by 1.8 MeV for twice the number of valence nucleons. Accurately accounting for the two-body interaction in the exotic medium is essential for calculations of exotic nuclei. The renormalization of a microscopic nucleon-nucleon interaction into the nuclear medium with a realistic basis and an appropriate target nucleus offers an improvement in our description of exotic nuclei, resulting in a decrease in the strength of the interaction and less binding in exotic nuclear systems.

## V. SUMMARY AND CONCLUSIONS

The microscopic nucleon-nucleon interaction N$^3$LO was renormalized using $v_{\mathrm{lowk}}$ and many-body perturbation theory to produce an effective interaction in the nuclear medium that could be used in a shell-model code. The renormalization was performed in three different bases: harmonic oscillator, core polarization, and Skyrme Hartree-Fock. The choice of basis can significantly affect the value of matrix elements, as shown in the comparisons of $pf$ neutron-neutron matrix elements for the stable $^{40}$Ca and the neutron-rich $^{34}$Si nuclei. The difference primarily results from the long tail of the radial wave functions relative to the harmonic oscillator wave function, especially for valence orbits bound by only a few hundred keV. The loosely bound orbits cause a reduction in the overall strength of the interaction, an effect that becomes magnified as full scale shell-model calculations are performed. Accounting for the properties of the orbits by using a realistic basis is essential for an accurate description of the nuclear interaction in exotic nuclei as determined by the renormalization of an $NN$ interaction, but $NNN$ forces must be included for accuracy at the level of 100 keV.

## ACKNOWLEDGMENTS

Support for this work was provided from National Science Foundation Grant No. PHY-0758099, from the Department of Energy (DOE) NNSA SSGF program through Grant No. DE-FC52-08NA28752, and from the DOE UNEDF-SciDAC through Grant No. DE-FC02-09ER41585.

[1] F. Nowacki and A. Poves, Phys. Rev. C **79**, 014310 (2009).
[2] M. Stanoiu *et al.*, Phys. Rev. C **78**, 034315 (2008).
[3] D. R. Entem and R. Machleidt, Phys. Rev. C **68**, 041001(R) (2003).
[4] S. K. Bogner, T. T. S. Kuo, and A. Schwenk, Phys. Rept. **386**, 1 (2003).
[5] B. A. Brown, T. Duguet, T. Otsuka, D. Abe, and T. Suzuki, Phys. Rev. C **74**, 061303(R) (2006).
[6] M. Hjorth-Jensen, T. T. S. Kuo, and E. Osnes, Phys. Rept. **261**, 125 (1995).
[7] J. Blomqvist and A. Molinari, Nucl. Phys. A **106**, 545 (1968).
[8] T. T. S. Kuo, F. Krmpotic, and Y. Tzeng, Phys. Rev. Lett. **78**, 2708 (1997).
[9] K. Ogawa *et al.*, Phys. Lett. B **464**, 157 (1999).
[10] NuShellX@MSU, B. A. Brown and W. D. M. Rae [http://www.nscl.msu.edu/~brown/resources/resources.html].
[11] L. Gaudefroy, W. Mittig *et al.* (private communication).